

The effect of electronic autoionization on vibrational branching ratio in (1 + 1′)-photon resonance-enhanced multiphoton ionization of H₂ molecules: dependence on laser intensity

Jainab Khatun and Krishna Rai Dastidar†

Department of Spectroscopy, Indian Association for the Cultivation of Science, Calcutta 700032, India

Received 27 May 1998, in final form 12 November 1998

Abstract. We have studied the laser intensity effect on the vibrational branching ratio (VBR) in (1 + 1′)-photon resonance-enhanced two-photon ionization of H₂ molecules, considering the electronic autoionization through the lowest autoionizing (AI) state of $^1\Sigma_g^+$ symmetry. In this *ab initio* calculation we have studied resonant two-photon transitions from the ground X $^1\Sigma_g^+$ ($v = 0, j = 0, 1$) state to the doubly excited autoionizing state of $^1\Sigma_g^+$ symmetry as well as to the electronic continuum ($H_2^+:X\ ^2\Sigma_g^+ + e$) of H₂ molecules via the resonant intermediate B $^1\Sigma_u^+(v = 4, j = 1, 2)$ levels. Transitions to two different continuum energies (−0.4500 au and −0.5853 au) have been considered; the first one is 1.36 eV above the dissociation threshold (−0.50 au) of the H₂⁺ ion and the second one is 0.048 eV above the $v^+ = 1$ vibrational level of the H₂⁺ ion in the ground state (X $^2\Sigma_g^+$). Parallel transitions through other intermediate near-resonant rovibrational levels $v = 0-3$ and $5-20$ with the allowed values of total angular momentum j of the B $^1\Sigma_u^+$ state have been included in the calculation. Besides the effect of interference of direct ionization with autoionization channels, we have considered here (i) the effects of mutual interference among parallel autoionization channels and that among parallel ionization channels via the near-resonant and resonant rovibrational levels of the B $^1\Sigma_u^+$ state and (ii) the effect of the two-photon coupling between intermediate rovibrational levels via the autoionizing state and the continuum in order to study the laser intensity dependence of vibrational distribution of H₂⁺ ions in the ground state. It has been shown that these two effects (channel interference effect and two-photon coupling effect) lead to non-Franck–Condon type VBR and the values differ from those obtained by considering the direct ionization channels alone. The laser intensity dependence of VBR is also different from that obtained by neglecting the autoionization channels. For transitions to two different continuum energies these effects become prominent at two different laser intensities. Furthermore, it has been found that the transitions through different intermediate resonant rotational levels of the B $^1\Sigma_u^+(v = 4)$ state give rise to different vibrational branching ratios.

1. Introduction

Experimental observations on resonance-enhanced multiphoton ionization (REMPI) of H₂ molecules have revealed several interesting features in the H₂⁺ ion signal and also in the photoelectron angular distribution [1]. To explain some of the experimental features [2], attempts were made [3] previously to study the (1 + 1′)-photon REMPI of H₂ molecules through the intermediate resonant levels $v = 4, j = 1$ and 2 of the B $^1\Sigma_u^+$ state. Parallel

† E-mail address: spkrdr@mahendra.iacs.res.in

ionizing transitions through nearby rovibrational levels of the $B^1\Sigma_u^+$ state have also been considered. In the previous work the intensity dependence of the vibrational branching ratio (VBR) and the photoelectron angular distribution (PEAD) has been studied by considering (i) the effect of interference of different ionizing channels through the resonant and near-resonant rovibrational levels of $B^1\Sigma_u^+$ state and (ii) the effect of coupling between these rovibrational levels via the continuum (i.e. Raman-like transition via the continuum). By considering the intensity dependence of these two effects on the vibrational branching ratio of the H_2^+ ion and the photoelectron angular distribution, we demonstrated that the VBR becomes non-Franck-Condon (FC) in nature and the PEAD varies in shape, as the laser intensity is increased. In those studies the effect of autoionization on the intensity dependence of VBR has been neglected.

It has been known that the autoionization adds an indirect contribution to the ionization process which interferes with the direct ionization [4–6], leading to a Fano-type [4] absorption profile and modifying the VBR. Recently it has been shown that the autoionization lineshape for $(1+1')$ -photon autoionization differs from that for single photon autoionization [7]. But for the simple Fano-type interference, VBR does not depend on the laser intensity. In the present work, we have studied $(1+1')$ -photon REMPI of H_2 molecules via $B^1\Sigma_u^+$ ($v=4; j=1, 2$) levels considering the effect of electronic autoionization through the lowest doubly excited autoionizing (AI) state of $^1\Sigma_g^+$ symmetry. We have also considered the parallel autoionizing and ionizing transitions via different near-resonant rovibrational levels ($v=0-3$ and $5-20$, with allowed values of total angular momentum j) of the $B^1\Sigma_u^+$ state. In this calculation, besides the Fano-type interference [4–7] between ionization and autoionization channels through each rovibrational level of the $B^1\Sigma_u^+$ state, we have included (i) the interference among parallel ionization channels and (ii) that among parallel autoionization channels through these intermediate rovibrational levels of the $B^1\Sigma_u^+$ state. The effect of Raman-like two-photon coupling between intermediate rovibrational levels via the ionization continuum as well as via the autoionizing state has also been considered. These above-mentioned effects become prominent with the increase in the laser intensity of the ionizing transition and we have shown here that the inclusion of the effects of channel interferences and the effect of two-photon couplings in the ionization process leads to significant intensity dependence of VBR. It has also been found that the VBR changes from FC to non-FC type with the increase in the laser intensity. The calculation by considering the non-FC nature of the dipole transitions (i.e. by considering the explicit dependence of dipole transition moments on the internuclear separation and on the photoelectron energies) and by considering the Fano-type interference effects [5, 6], could not explain the observed strong deviation of VBR [2] from FC nature. To explain this feature of significant deviation of VBR from FC nature, we have included the above-mentioned effects in this paper. These effects depend on the laser intensity and we have shown that the VBR becomes non-FC in nature with the increase in the laser intensity. To our knowledge the inclusion of the channel interference effects and the two-photon coupling effects (as mentioned above) on the autoionization process is a new attempt which, we find, shows that VBR deviates strongly from FC nature. Furthermore, we have shown that the VBR depends on the rotational quantum number of the intermediate resonant rovibrational levels. This feature has also been previously observed [2] in the experimental study on $(3+1)$ -photon REMPI of H_2 via the $B^1\Sigma_u^+$ state. But further experimental investigation is needed to explore this feature of dependence of VBR on the laser intensity of the ionizing transition.

We have done the calculation for transitions to two different continuum energies -0.5853 au and -0.4500 au and have shown that for these two transitions the VBR becomes non-FC in nature at two different laser intensity regimes.

For transitions close to the ionization threshold (continuum energy -0.5853 au, i.e. 0.048 eV above the $v^+ = 1$ vibrational level of the ground state $1s\sigma_g$ of the H_2^+ ion) the presence

of excited Rydberg autoionizing states can give rise to rovibrational autoionization, and the coupling of doubly excited autoionizing state to these Rydberg levels can lead to dissociation producing excited atoms. In this paper, we have considered the electronic autoionization via the lowest doubly excited state of $^1\Sigma_g^+$ symmetry (dominant configuration: $\sigma_u(1s)\sigma_u(1s)$) which is the fastest autoionization process [2, 8] and neglected the rovibrational autoionization effects through excited Rydberg levels. It is well known that the rovibrational autoionization obeys the propensity rule $\Delta v = -1$. Therefore, for transition to the continuum energy -0.5853 au which is just above the $v^+ = 1$ level of the H_2^+ ion, the vibrational autoionization from the $v = 1$ and 2 levels of excited Rydberg states which are above the $v^+ = 0, 1$ levels of the H_2^+ ion may play a role. But only the Rydberg states with large principal quantum numbers $n > 7$ can have lower vibrational levels close to the ionization threshold. Therefore, it is expected [8] that the photo-excitation probability from the $B^1\Sigma_u^+$ state (dominant configuration: $\sigma_g(1s)\sigma_u(1s)$) to the doubly excited state which has got $\sigma_u(1s)\sigma_u(1s)$ as the dominant configuration will be larger than the photo-excitation probability to the Rydberg levels with large principal quantum numbers ($n > 7$). In this paper we demonstrate the role of electronic autoionization on this REMPI process neglecting the rovibrational autoionization. But one can also include the effect of rovibrational autoionization in a similar fashion when this channel becomes important.

For transition to the continuum (at -0.4500 au, i.e. 1.36 eV) above the dissociation threshold of the H_2^+ ion in the ground state, we have considered electronic autoionization through the lowest AI state $^1\Sigma_g^+(1)$ only. But the contribution from the first excited AI state $^1\Sigma_g^+(2)$ cannot be ruled out. It is found that for the lowest AI state the turning point for this continuum energy (-0.45 au) is 2.2 au and that for the first excited AI state is 3.2 au [10]. Since the turning point for the lowest AI state is well within the FC region for the H_2^+ ion, it is expected that the contribution from this state will be greater than that from the first excited AI state, in particular for the lower vibrational levels ($v^+ < 10$) of the H_2^+ ion. Furthermore, as mentioned above, electronic autoionization from the lowest AI state is the fastest autoionization process [14]. Therefore, considering these two facts, one can expect that the contribution from the lowest AI state will be much greater than that from the first excited AI state. Nevertheless, further calculation is required for quantitative comparison.

For the transition to the continuum above the dissociation threshold of H_2^+ ion, we have not included contribution from the autoionization to the dissociative continuum of H_2^+ ion. To calculate the total ionization rate the contribution from the dissociative autoionization should, in principle, be included along with the contribution from the bound vibrational levels of the ion. If the contribution from the dissociative autoionization modifies the total ionization rate, the absolute values of vibrational branching ratio may change, but the relative ion yields to different vibrational levels will not be affected. Moreover the two main conclusions drawn in this work, namely that the VBR depends on the laser intensity and that the VBR changes from FC to non-FC type with increase in laser intensity, will remain unchanged; only the finer details of intensity dependence of VBR may change. We feel however that this aspect of the photoionization process merits further detailed study.

2. Transition schematics

To study the $(1 + 1')$ -photon REMPI of H_2 molecules, we have chosen two transition schemes for the lower step resonant excitation: (i) the single-photon resonant excitation from the ground $X^1\Sigma_g^+(v = 0; j = 0) \rightarrow B^1\Sigma_u^+(v = 4; j = 1)$ level, i.e. the R(0) transition and (ii) the single-photon resonant excitation from the ground $X^1\Sigma_g^+(v = 0; j = 1) \rightarrow B^1\Sigma_u^+(v = 4; j = 2)$ level, i.e. the R(1) transition. Here v and j are the vibrational and total angular momentum

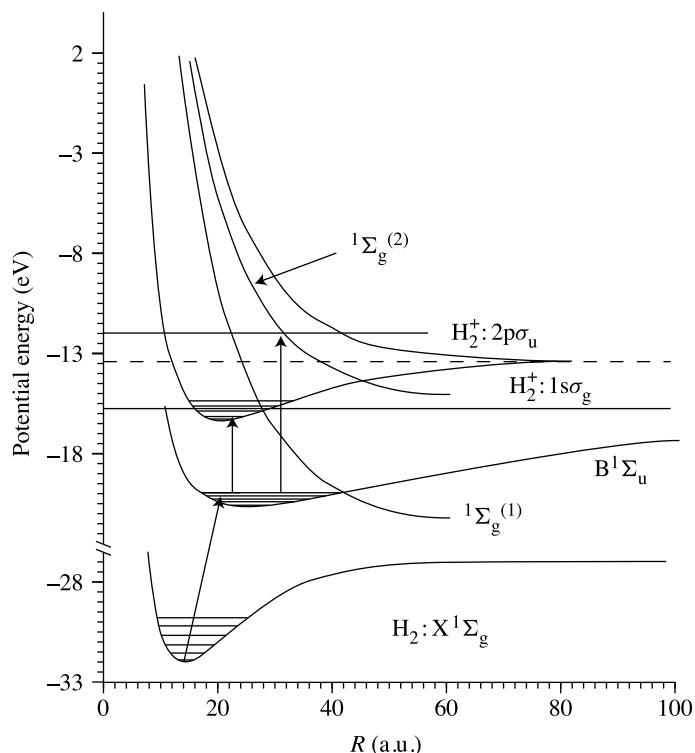


Figure 1. Potential energy curves for H₂ showing ground X¹Σ_g⁺, excited B¹Σ_u⁺ and two doubly excited autoionizing (1¹Σ_g⁺(1) and 1¹Σ_g⁺(2)) states. Two lowest potential energy curves for H₂⁺: 1σ_g and 2pσ_u have also been shown. The horizontal dashed line shows the dissociation threshold for the H₂⁺ ion. Two horizontal solid lines show the two continuum energies to which the transitions have been considered.

quantum number respectively. In both cases the intensity of the first laser connecting the ground state (X¹Σ_g⁺) to the resonant intermediate state (B¹Σ_u⁺) by the single photon transition has been considered to be weak enough to neglect the ac-Stark effect due to the single-photon coupling between these two bound levels. By the second photon the molecule is being excited from the resonant level either to the lowest autoionizing state (1σ_u²) or directly to the ionization continuum (X²Σ_g⁺: H₂⁺ + e) (figure 1). For the transition to the autoionizing state we have included the effect of dissociation as well as autoionization, using the nuclear wavefunctions obtained by solving the nuclear Schrödinger equation for the complex potential of this antibonding state. We have considered here transitions to two continuum energies (−0.5853 au and −0.4500 au). The intensity of the laser causing the ionizing transition is varied to study the dependence of VBR on the laser intensity. The photon energies required for the transitions to these two continua from the B¹Σ_u⁺ state are around 4 eV and 7.68 eV respectively. In addition to the resonant ionization and autoionization channels through B¹Σ_u⁺ (v = 4; j = 1, 2) levels, we have also considered the near-resonant ionization and autoionization channels through other rovibrational levels v = 0–3 and v = 5–20 (with the allowed values of j) of the B¹Σ_u⁺ state. It is obvious that for the R(1) transition scheme both the angular momentum quantum numbers j = 0 and 2 are allowed for near-resonant channels. But for the R(0) transition scheme only the j = 1 angular momentum is allowed for near-resonant transition. Furthermore, the effect of alignment of the molecules in the intermediate

levels has also been taken into consideration. The transitions through intermediate levels with different values of magnetic quantum numbers M_i (which is the projection of the total angular momentum j of the intermediate state on the laser polarization axis) have been treated as separate transitions. For the R(0) transition scheme the possible values of magnetic quantum number for the intermediate levels are $M_i = -1, 0, +1$, but the allowed value of magnetic quantum number is 0, due to the $\Delta M = 0$ selection rule. Similarly the allowed values of M_i are $-1, 0, +1$ for the R(1) transition scheme. To obtain the ionization rate we have summed over the contributions from ionization via intermediate levels with different values of magnetic quantum numbers. It is to be mentioned here that for the transition to the continuum energy -0.5853 au, vibrational branchings of the H_2^+ ion in $v^+ = 0$ and 1 levels are energetically accessible. But for the transition to the continuum energy -0.4500 au, which is 1.36 eV above the dissociation limit of the H_2^+ ion, all the vibrational levels of the H_2^+ ion are accessible. Furthermore, the dissociation continua lying within 1.36 eV above the dissociation threshold of the H_2^+ ion are also accessible. For this calculation, we have not considered the near-resonant transition through the $C^1\Pi_u$ state, because of the fact that the transition amplitude from this state to the autoionizing state of $1^1\Sigma_g^+$ symmetry is much less than that for transition from the $B^1\Sigma_u^+$ state.

3. Theory

Let H be the total Hamiltonian of the system (molecule + radiation field) and be given as

$$H = H_M + H_R + H_{int}, \quad (1)$$

where H_M and H_R are the free Hamiltonians for the molecule and radiation field respectively and H_{int} is the matter–radiation interaction Hamiltonian. Hence the resolvent operator equation can be written as

$$(Z - H)G(Z) = 1, \quad (2)$$

where $G(Z)$ is the resolvent operator and Z is a complex variable. Starting from this equation we can obtain equations for the matrix elements of resolvent operator as

$$(Z - E_g)G_{gg} - \sum_{i=i_1 \dots i_n} D_{gi}G_{ig} = 1 \quad (3a)$$

$$(Z - E_{i_1})G_{i_1g} - \int D_{i_1c}G_{cg} dE_c - D_{i_1g}G_{gg} - D_{i_1a}G_{ag} = 0 \quad (3b)$$

$$(Z - E_{i_2})G_{i_2g} - \int D_{i_2c}G_{cg} dE_c - D_{i_2g}G_{gg} - D_{i_2a}G_{ag} = 0 \quad (3b')$$

⋮

$$(Z - E_{i_n})G_{i_ng} - \int D_{i_nc}G_{cg} dE_c - D_{i_ng}G_{gg} - D_{i_na}G_{ag} = 0 \quad (3b'')$$

$$(Z - E_a)G_{ag} - \int V_{ac}G_{cg} dE_c - \sum_{i=i_1 \dots i_n} D_{ai}G_{ig} = 0 \quad (3c)$$

$$(Z - E_c)G_{cg} - V_{ac}G_{cg} - \sum_{i=i_1 \dots i_n} D_{ci}G_{ig} = 0, \quad (3d)$$

where the matrix elements of the resolvent operator $G_{pq} = \langle p|G|q \rangle$ are written in the basis of product states, i.e. $|g\rangle|n\rangle$, $|i\rangle|n-1\rangle$, $|a\rangle|n-2\rangle$ and $|c\rangle|n-2\rangle$, for the total (molecule +

photon) system. Here $|n\rangle$ are the photon number states and $|g\rangle$, $|i\rangle$, $|a\rangle$ and $|c\rangle$ are the molecular ground, intermediate, autoionizing and continuum states respectively. Here $E_g = \epsilon_g + n\hbar\omega$, $E_i = \epsilon_i + (n-1)\hbar\omega$, $E_c = \epsilon_c + (n-2)\hbar\omega$, $E_a = \epsilon_a + (n-2)\hbar\omega$, are the energies of the product states where ϵ are the energies of the bare molecular states. For solving these equations we replaced $Z - E_g$ by Z' such that $Z - E_p$ can be written as $Z' + \delta_p$ where δ_p is the detuning from the product state $|p\rangle$. Hence δ_p is non-zero for non-resonant levels. Therefore, solving for matrix elements of resolvent operators one can formally obtain $G_{gg}(Z')$ as

$$G_{gg}(Z') = \frac{1}{(Z' - Z_0)}, \quad (4)$$

where

$$Z_0 = \sum_{i=i_1 \dots i_n} \frac{|D_{gi}|^2}{Z' + \delta_i - s_i + \frac{i}{2}\gamma_i - \frac{|Q_i|^2}{A} - \sum_{j=i_1 \dots i_n, j \neq i} \frac{|T_{ij}|^2}{B_j}} + \sum_{i=i_1 \dots i_n} \sum_{j=i_1 \dots i_n, j \neq i} \frac{D_{gi} D_{jg} T_{ij}}{\left[Z' + \delta_i - s_i + \frac{i}{2}\gamma_i - \frac{|Q_i|^2}{A} - \sum_{p=i_1 \dots i_n, p \neq i} \frac{|T_{ip}|^2}{B_p} \right] B_j}, \quad (5)$$

where

$$\begin{aligned} Q_i &= D_{ia} + \int \frac{D_{ic} V_{ca}}{(Z' - E'_c)} dE'_c \\ A &= Z' + \delta_a - s_a + \frac{i}{2}\gamma_a \\ B_i &= Z' + \delta_i - s_i + \frac{i}{2}\gamma_i - \frac{|Q_i|^2}{A} \\ T_{ij} &= \frac{Q_i Q_j^*}{A} + \int \frac{D_{ic} D_{cj}}{(Z' - E'_c)} dE'_c. \end{aligned}$$

Here D_{pq} are the dipole transition moments between the product states $|p\rangle$ and $|q\rangle$. s_i and γ_i are the ac-Stark shift and width of the intermediate level $|i\rangle$ due to the radiation coupling with the continuum. V_{ac} is the configuration interaction matrix element between the autoionizing state and the continuum; $\gamma_a (= 2\pi |V_{ac}|^2)$ is the autoionization width. The real and imaginary parts of the first and second terms of T_{ij} correspond to the shifting and broadening of different intermediate levels due to Raman-like couplings via the autoionizing state and via the continuum respectively. It is obvious that Q_i can be expressed in terms of Fano asymmetry parameters [4] and gives contributions from the interference of autoionization channel with the direct ionization channel from the intermediate level $|i\rangle$. It is implicit that all the dipole transition moments D_{pq} connecting the intermediate levels to the other levels are functions of M_i . Hence all the shifts and widths (s_i , γ_i , T_{ij} etc) which involve these dipole transition moments are functions of M_i . The matrix element of the time evolution operator $U_{pq}(t)$ is obtained by the inverse Laplace transform of the corresponding matrix element of the resolvent operator $G_{pq}(Z)$. $|U_{pq}(t)|^2$ gives the population in the state $|p\rangle$ at time t . Hence the ionization probability in the weak field limit can be written as $P(t) = 1 - |U_{gg}(t)|^2$. Therefore the rate of ionization $\frac{dp}{dt} = -\frac{d}{dt} |U_{gg}(t)|^2$, in the limit $t \rightarrow 0$, reduces to

$$\frac{dp}{dt} = -2\text{Im } Z_0. \quad (6)$$

Here Z_0 is evaluated at $Z' = 0$, i.e. the pole approximation has been used to evaluate the ionization rate. From the expression of Z_0 it is obvious that the first term gives the sum of the contributions of ionization (including ionization–autoionization interference) via the

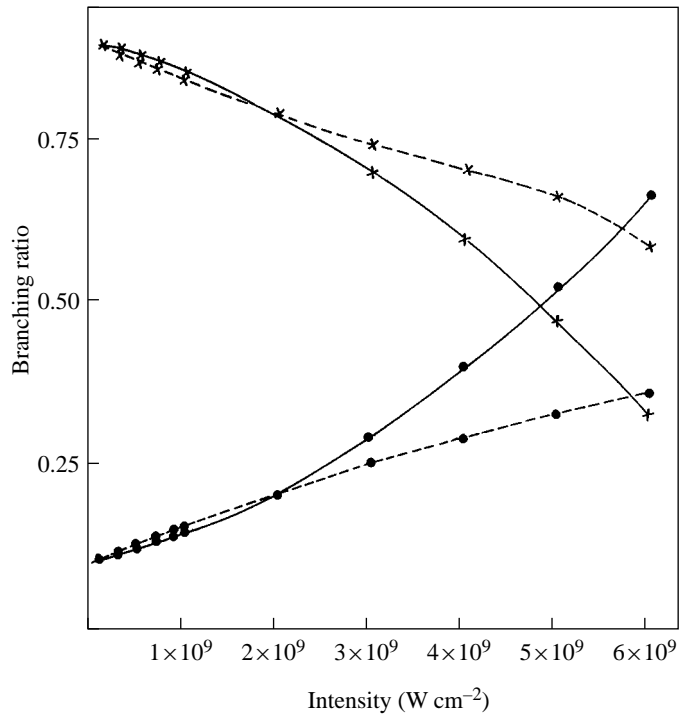


Figure 2. Vibrational branching ratios as a function of laser intensity with and without autoionization for both the $v^+ = 0$ and $v^+ = 1$ levels. Calculated points have been shown by solid circles for $v^+ = 0$ and by crosses for $v^+ = 1$ level. These points have been joined by solid curves for the calculation with autoionization and by dashed curves for the calculation without autoionization. The $R(0)$ transition scheme has been considered. The continuum energy is -0.5853 au.

Table 1. Population factors for transition from the $v = 4, j = 2$ level of the $B^1\Sigma_u^+$ state to the $v = 0 \rightarrow 11, j = 2$ levels of $X^2\Sigma_g^+$ state of the H_2^+ ion (a: calculated following the method as given in [12] and b: calculated following the method as in [13]).

v^+	Population distribution factor	
	a	b
0	0.0166	0.0118
1	0.1119	0.0860
2	0.1502	0.1241
3	0.0004	0.0003
4	0.1365	0.1300
5	0.0360	0.0367
6	0.4090	0.4447
7	0.1194	0.1399
8	0.0156	0.0199
9	0.0025	0.0034
10	0.0001	0.0002
11	0.0006	0.0009

resonant and all the near-resonant levels, while the second term gives the total contribution from the mutual interference among ionization channels and that from the mutual interference

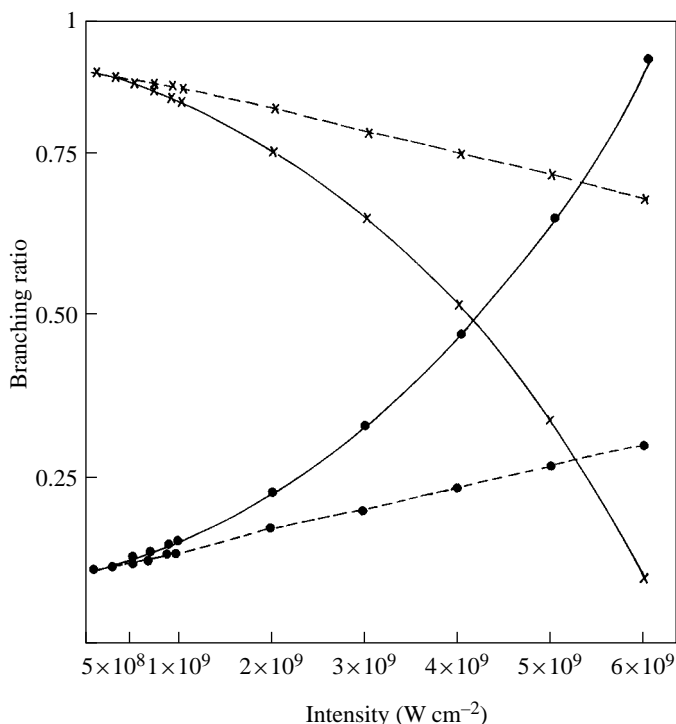


Figure 3. Same as figure 2 considering the R(1) transition scheme.

among autoionization channels. The total ionization rate $\frac{dp}{dt}$ can be expressed as the sum of the vibrationally resolved rates, i.e.

$$\frac{dp}{dt} = \sum_{v^+} \frac{dp(v^+)}{dt} \quad (7)$$

where v^+ is the vibrational quantum number of the molecular ion. Hence the branching ratios for the vibrational distribution can be written as

$$B(v^+) = \frac{\frac{dp(v^+)}{dt}}{\sum_{v^+} \frac{dp(v^+)}{dt}} \quad (8)$$

It is implicit that the vibrationally resolved rate has been obtained by summing over rates as a function of M_i , the magnetic quantum number of the intermediate levels.

4. Calculation

The electronic wavefunctions for the ground and intermediate states of H_2 and the ground state of H_2^+ ion and the bound-bound dipole transition moments were obtained from our previous calculations [3]. The nuclear vibrational wavefunctions for the bound states were obtained by using Cooley's method [9]. The final dipole transition moments were obtained by integrating the product of electronic dipole transition moment (as a function of internuclear separation), the initial nuclear wavefunction and the final nuclear wavefunction, over the nuclear coordinates. The electronic wavefunctions for the autoionizing state and hence the real and imaginary parts of the complex potential for the AI state were obtained from previous calculations [10]. To

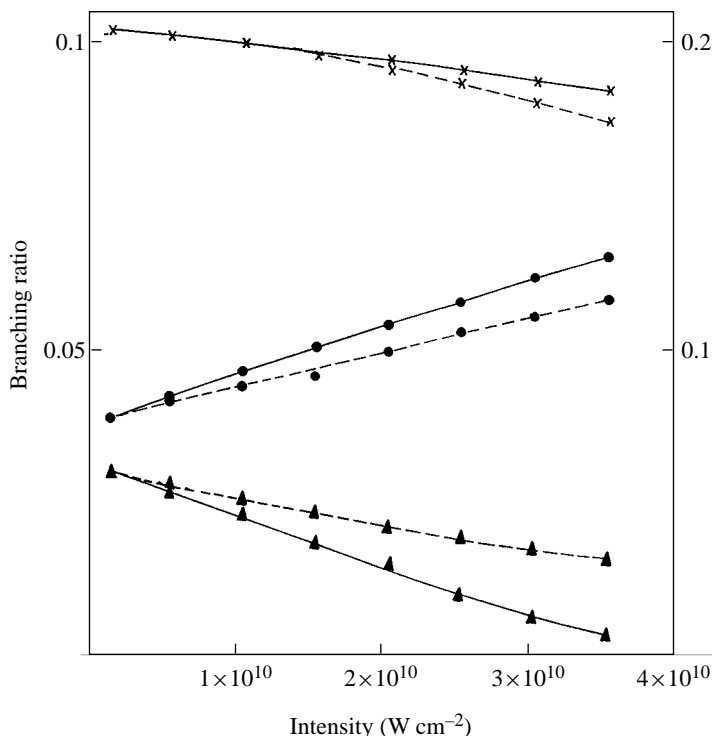


Figure 4. VBR as a function of laser intensity with autoionization (solid curve) and without autoionization (dashed curve) for $v^+ = 0$ (solid circles), $v^+ = 1$ (crosses) and $v^+ = 2$ (solid triangles) for the R(0) transition scheme. The left ordinate scale is for $v^+ = 0$ and 2 and the right ordinate scale is for $v^+ = 1$. The continuum energy is -0.4500 au.

get the nuclear wavefunction for the complex potential, the modified Cooley's method [11] was used. The configuration interaction (V_{ac}) coupling term (electronic) between the AI state and the continuum and the bound–continuum dipole transition moments (electronic) were evaluated as a function of internuclear separation and the photoelectron energy. The final matrix elements were obtained by integrating over nuclear coordinates, the integrand being the product of initial nuclear wavefunction, final nuclear wavefunction and the bound–continuum interaction matrix element. Finally the vibrational branching ratios $B(v^+)$ for $(1 + 1')$ -photon autoionization were evaluated as a function of laser intensity. We have also calculated VBRs by neglecting the effect of autoionization, i.e. by considering the direct photoionization channels only. In this paper we have presented the values of VBR calculated using the autoionization width obtained from our previous calculation [10]. A sample calculation using more recent values of width [14, 15] shows that the change in the values of VBR is negligible (1% or less).

5. Results and discussions

Figure 2 gives the VBRs as a function of laser intensity for the $v^+ = 0$ and $v^+ = 1$ levels of the H_2^+ ion ($X^2\Sigma_g^+$) for the R(0) transition scheme. Values of VBR calculated with autoionization and without autoionization have been shown by points on the figure and lines have been drawn to join the points. Figure 3 shows similar results for the R(1) transition scheme. The continuum energy -0.5853 au is just above the $v^+ = 1$ level of H_2^+ ion and hence the molecular ions are

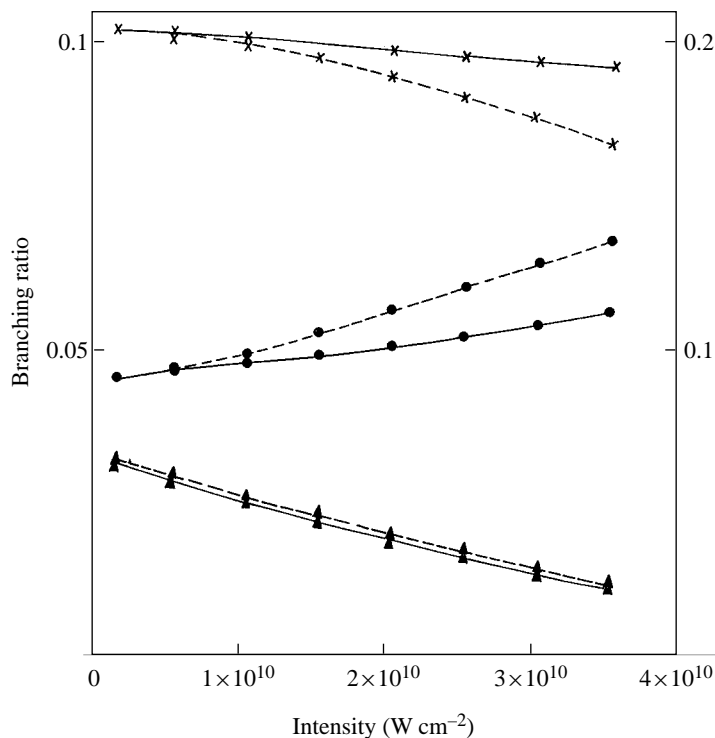


Figure 5. Same as figure 4, but the lower step excitation is the R(1) transition.

produced only to the $v^+ = 0$ and 1 levels. Comparison of figures 2 and 3 shows that the effect of autoionization is not very strong for laser intensity less than $1 \times 10^9 \text{ W cm}^{-2}$ for either of the transition schemes. But with the increase in laser intensity the effect of autoionization starts being prominent from laser intensity $1 \times 10^9 \text{ W cm}^{-2}$ for the R(1) transition scheme and from laser intensity $2 \times 10^9 \text{ W cm}^{-2}$ for the R(0) transition scheme. It is found that the VBR is very close to the FC values at the laser intensity $1 \times 10^8 \text{ W cm}^{-2}$. But with the increase in laser intensity the VBR shows non-FC-type distribution, i.e. branching to the $v^+ = 0$ level increases and the difference in the values of VBR obtained with and without autoionization becomes significant. This is because of the fact that in the lower intensity regime only the interference of autoionization with direct ionization contributes to the ionization rate. But with the increase in the laser intensity the effect of mutual interference of autoionization channels (resonant and near-resonant) and the effect of two-photon coupling between these intermediate levels via autoionizing state become prominent, leading to a significant deviation of VBR from the FC values. These effects also lead to vibrational branching ratios which are different from those obtained by considering the direct ionization channels only (i.e. neglecting autoionization). It is also found that the difference between the values of VBR obtained with and without autoionization increases with the laser intensity. This demonstrates the prominence of the above-mentioned effects at different laser intensities.

It is also found that at a particular laser intensity the VBR for the R(1) transition scheme is different from that for the R(0) transition scheme. This is due to the fact that the number of channels contributing to ionization in the R(1) transition scheme is double that contributing to ionization in the R(0) transition scheme. This causes the autoionization effect to be more

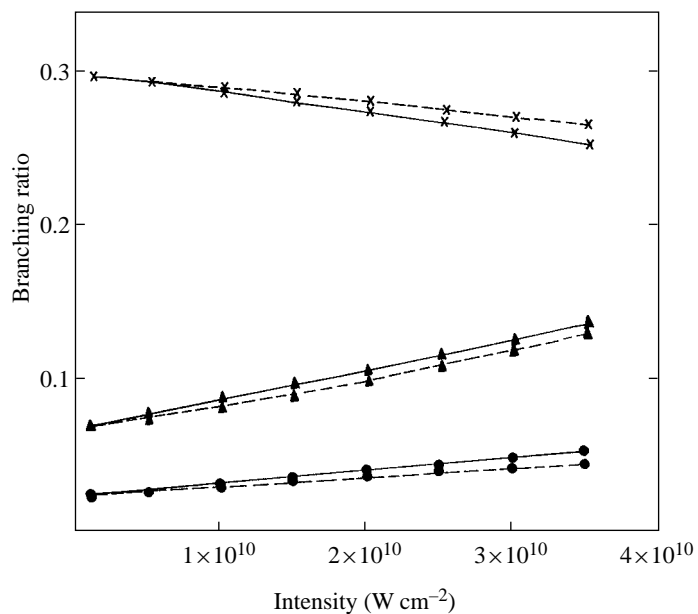


Figure 6. Same as figure 4, but for vibrational levels $v^+ = 5$ (solid circles), $v^+ = 6$ (crosses) and $v^+ = 7$ (solid triangles). The left ordinate scale is for $v^+ = 5$ and 7 and the right ordinate scale is for $v^+ = 6$.

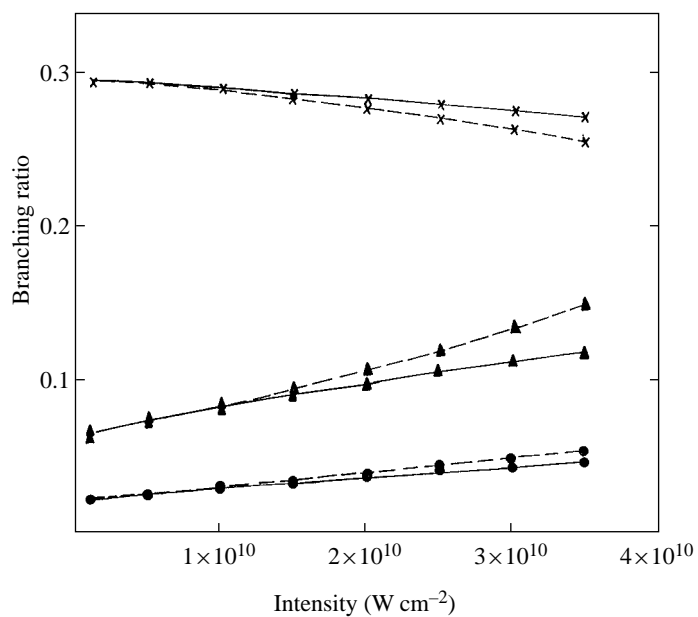


Figure 7. Same as figure 4, but the lower step excitation is the R(1) transition.

prominent for the R(1) transition scheme than for the R(0) transition scheme.

For transition to higher continuum energy at -0.4500 au (which is 1.36 eV above the dissociation threshold of the H_2^+ ion), all the vibrational levels and the dissociation continua

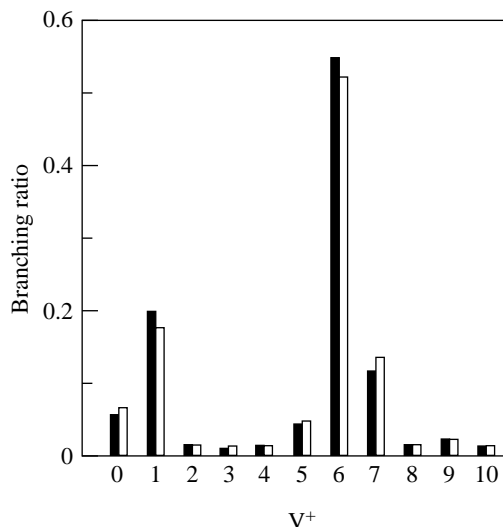


Figure 8. Histograms for VBR with and without autoionization (solid bar without autoionization and open bar with autoionization) for the R(1) transition scheme. The continuum energy is -0.4500 au.

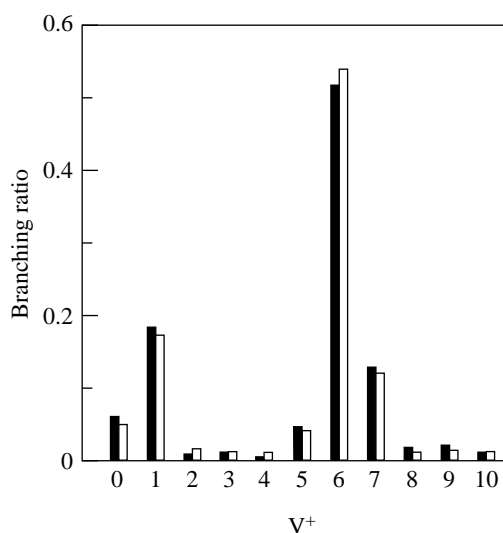


Figure 9. Same as in figure 8 considering the lower step excitation as the R(0) transition scheme.

of H_2^+ ion lying below this continuum energy are accessible. However, in this paper, we have considered the contribution from the autoionization to the bound vibrational levels of the H_2^+ ion only. Figures 4 and 5 show the intensity dependence of VBR (with and without autoionization) for the R(0) and R(1) transition schemes respectively. VBR for $v^+ = 0, 1$ and 2 have been shown in these two figures. Figures 6 and 7 give similar results for $v^+ = 5, 6$ and 7. We have calculated the VBRs up to $v^+ = 17$, but we have omitted all those VBRs for which the difference in values of VBR with and without autoionization is very small. It is found that, for both transition schemes, branching to $v^+ = 6$ and $v^+ = 1$ is favoured much more than that in other vibrational levels of the H_2^+ ion. The FC population distribution in different vibrational levels of the H_2^+ ion has been given in table 1. The values were calculated in two different ways; (i) considering only the square of the overlap of initial vibrational wavefunction for $v = 4, j = 2$ of the $B^1\Sigma_u^+$ state of H_2 and final vibrational wavefunctions

for $v^+ = 0 \rightarrow 17$, $j = 2$ of the $X^2\Sigma_g^+$ state of the H_2^+ ion [12] and (ii) considering the ratio of the square of the overlap and the photoelectron energy corresponding to the particular vibrational level of the H_2^+ ion [13]. To obtain population factors, individual FC factors have been divided by the total, i.e. sum, of the FC values. Comparison of figures 4–7 with table 1 shows that VBRs are non-FC in nature for laser intensity greater than $1 \times 10^{10} \text{ W cm}^{-2}$ although qualitatively the $v^+ = 6$ level is the most favoured level for branching for both the FC and non-FC distributions. For laser intensity greater than $1 \times 10^{10} \text{ W cm}^{-2}$, redistribution of vibrational branching occurs, around the $v^+ = 6$ and $v^+ = 1$ levels of H_2^+ ion. Moreover, the difference in values of VBR with and without autoionization increases with the increase in laser intensity. This difference demonstrates the effect of autoionization. A similar effect has also been shown (in figures 2 and 3) for the transition to the lower continuum. Comparison of these four figures (4–7) also shows that at a particular laser intensity, VBR for the R(1) transition is different from that for the R(0) transition, and the inclusion of autoionization affects the VBR differently for these two transition schemes. To demonstrate this effect, the bar diagrams for VBR with and without autoionization for the R(1) and R(0) transition schemes at laser intensity $3 \times 10^{10} \text{ W cm}^{-2}$ have been given in figures 8 and 9 respectively. Figure 8 shows that for the R(1) transition scheme, the inclusion of autoionization tends to decrease the VBR for $v^+ = 6$ and 1 levels, whereas the effect is reversed for branching to other vibrational levels of the H_2^+ ion. For the R(0) transition scheme (figure 9), the effect of autoionization leads to increase in VBR for $v^+ = 6$ level and to decrease the same for other vibrational levels of the H_2^+ ion.

In conclusion, we have shown that autoionization affects the vibrational distribution of H_2^+ ions in $(1 + 1')$ -photon REMPI of H_2 molecules and the VBR varies with the laser intensity of the ionizing transition. This is due to the fact that (i) interference of autoionization with the direct photoionization gives an indirect contribution to the ionization, (ii) the mutual interference among autoionizing transitions through resonant and near-resonant rovibrational levels modifies the net autoionization and (iii) the coupling of the intermediate rovibrational levels via autoionizing state (i.e. Raman-like two-photon coupling) affects the ionization rate. Towards the lower intensity regime, only the first one contributes, but with increase in laser intensity the last two effects become prominent leading to significant deviation of VBR from that obtained considering only the direct ionization channels. It is found that for transitions to different continuum energies, this feature of deviation of VBR obtained with autoionization from that obtained without autoionization shows up at different laser intensities. It has also been shown that, as in our previous calculation [3] considering direct ionization channels only, VBR for autoionization obtained in this paper are different for the R(1) and R(0) transition schemes.

Acknowledgments

This work has been sponsored and supported by the Department of Science and Technology, Government of India, under Project no SP/S2/L-20/90 and SP/S2/L-09/94. JK is thankful to the Council of Scientific and Industrial Research, New Delhi, for support.

References

- [1] Pratt S T, Dehmer P M and Dehmer J L 1987 *J. Chem. Phys.* **86** 1727
Normand D, Cornaggia C and Morrelec J 1986 *J. Phys. B: At. Mol. Phys.* **19** 2881
Zavriyev A, Bucksbaum P H, Squier J and Salane F 1993 *Phys. Rev. Lett.* **70** 1077
Burnett K, Reed V C and Knight P L 1993 *J. Phys. B: At. Mol. Opt. Phys.* **26** 561

- [2] Verschuur J W J and van Linden van den Heuvell H B 1989 *Chem. Phys.* **129** 1
- [3] Khatun J, Sanyal S and Rai Dastidar K 1994 *Phys. Rev. A* **49** 4765
Khatun J and Rai Dastidar K 1995 *Phys. Rev. A* **52** 2971
Khatun J and Rai Dastidar K 1996 *Phys. Rev. A* **53** 4326
- [4] Fano U 1961 *Phys. Rev. A* **124** 1866
- [5] Dixit S N, Lynch D L, Mckoy B V and Hazi A U 1989 *Phys. Rev. A* **40** 1700
- [6] Hickman A P 1987 *Phys. Rev. Lett.* **59** 1553
Cornaggia C, Giusti-Suzor A and Jungen Ch 1987 *J. Chem. Phys.* **87** 3934
- [7] Adhya L and Rai Dastidar K 1994 *Phys. Rev. A* **50** 3537
- [8] Chupka W A 1987 *J. Chem. Phys.* **87** 1488
Verschuur J W J 1989 *PhD Dissertation* FOM-Institute for Atomic and Molecular Physics, Amsterdam ch 6
- [9] Cooley J W 1961 *Math. Comput.* **15** 363
- [10] Gubermann S L 1983 *J. Chem. Phys.* **78** 1404
Rai Dastidar K and Rai Dastidar T K 1979 *J. Phys. Soc. Japan* **46** 1288
- [11] Lane N F and Geltman S 1967 *Phys. Rev.* **160** 53
- [12] Dunn G H 1966 *J. Chem. Phys.* **44** 2592
- [13] Anderson S L, Kubiak G D and Zare R N 1984 *Chem. Phys. Lett.* **105** 22
- [14] Tennyson J 1996 *At. Data Nucl. Data Tables* **64** 253
- [15] Collins L A, Schneider B I, Lynch D L and Noble C J 1995 *Phys. Rev. A* **52** 1310 and references therein